

Effect of external pressure on the magnetism of $\text{UCo}_{0.98}\text{Fe}_{0.02}\text{Al}$

N. V. Mushnikov* and T. Goto†

Institute for Solid State Physics, University of Tokyo, 5-1-5 Kashiwanoha, Kashiwa, Chiba 277-8581, Japan

A. V. Andreev

Institute of Physics, Academy of Sciences, Na Slovance 2, 18221 Prague 8, Czech Republic

V. Sechovský

Department of Electronic Structures, Charles University, Ke Karlovu 5, 121 16 Prague 2, Czech Republic

H. Yamada

Faculty of Science, Shinshu University, Asahi, Matsumoto 390-8621, Japan

(Received 7 April 2002; published 30 August 2002)

UCoAl is an itinerant $5f$ -electron metamagnet. Just 2% substitution of Fe for Co in UCoAl stabilizes a ferromagnetic ground state. We studied the temperature and field dependences of the magnetization of a $\text{UCo}_{0.98}\text{Fe}_{0.02}\text{Al}$ single crystal under hydrostatic pressures up to 1.2 GPa. The reentrant metamagnetism of the UCoAl type was observed under pressures above 0.4 GPa. The experimental data have been analyzed based on the theory of itinerant electron metamagnetism, which considers anisotropic thermal fluctuations of the magnetic moment.

DOI: 10.1103/PhysRevB.66.064433

PACS number(s): 75.30.Kz, 75.30.Cr

I. INTRODUCTION

Itinerant electron metamagnetism, i.e., a first-order field-induced transition of an itinerant electron system from the paramagnetic to the ferromagnetic state, is a peculiar phenomenon that originates from the special shape of the density of states near the Fermi level.¹ The family of itinerant electron metamagnets is relatively small and consists of few intermetallic systems.² The only $5f$ itinerant electron metamagnet known is the UCoAl compound, which crystallizes in the hexagonal ZrNiAl-type structure.³ The ground state of UCoAl is paramagnetic.^{4,5} The magnetic susceptibility is exchange enhanced and exhibits a broad maximum as a function of temperature. In a magnetic field of approximately 0.6 T applied along the c axis, this compound undergoes a metamagnetic transition to a ferromagnetic state with a U magnetic moment of $0.3\mu_B$.⁵⁻⁷

The metamagnetic transition in UCoAl is sensitive to pressure.^{8,9} The critical field of the transition B_c increases with pressure at a rate 2.6 T/GPa. The observed pressure effect on the magnetism of UCoAl is well described with the spin-fluctuation theory for strongly anisotropic itinerant magnetic systems.⁹⁻¹¹ The magnetic phase diagram in the T - P plane was constructed using experimental data.⁹ However, the theoretical phase diagram calculated for itinerant metamagnets¹² includes not only the metamagnetic and paramagnetic phases but also the spontaneous ferromagnetic state that cannot be observed in UCoAl under any hydrostatic pressure condition. According to our estimation, the ferromagnetic phase will be stabilized in UCoAl by applying an effective negative pressure of more than -0.25 GPa.⁹

On the other hand, the ferromagnetic ground state can be easily achieved in UCoAl by a relatively small substitution of U by Y or Lu (Refs. 13 and 14) and Al by Ga (Ref. 15) or In.¹⁶ Similarly, just 2% doping of the Co sublattice by Ru or

Fe switches the specific metamagnetic phenomena in UCoAl to the ferromagnetism.^{17,18} Such a transformation is mainly due to a change in the hybridization of the uranium $5f$ states and the s , p , d electron states of other neighboring atoms rather than by a single volume effect.³ By applying pressure, reentrant metamagnetism was observed for the $\text{UCo}(\text{Al}_{1-x}\text{Ga}_x)$ (Ref. 19) and $(\text{U}_{1-x}\text{Y}_x)\text{CoAl}$ (Ref. 20) compounds, which exhibit a ferromagnetic ground state at ambient pressure. These studies were performed, however, on only available polycrystalline samples. Because of the strong uniaxial magnetic anisotropy, the metamagnetic transition on the magnetization curves measured on polycrystalline samples is strongly broadened, which prevents a reasonable comparison between the experiment and the theory. In this work we study the evolution of the magnetic properties of a single crystal of $\text{UCo}_{0.98}\text{Fe}_{0.02}\text{Al}$ with applied hydrostatic pressure, including the pressure-induced transition from the ferromagnetic to the metamagnetic state. The results are discussed in the framework of the theory of anisotropic spin fluctuations in comparison with data available for the stoichiometric UCoAl.

II. EXPERIMENTAL DETAILS

A single crystal of $\text{UCo}_{0.98}\text{Fe}_{0.02}\text{Al}$ was grown by the modified Czochralski method from the melt of stoichiometric amounts of the constituent elements (U of 99.95% purity, Co and Fe of 99.99% purity, and Al of 99.9999% purity) in a tetra-arc furnace. The sample of nearly cubic shape of the size of ~ 1.8 mm³ and mass of 60 mg was spark erosion cut perpendicular to the principal axes.

For magnetization measurements under high pressure, the sample was compressed in a Teflon capsule filled with a liquid pressure-medium, a mixture of two types of Fluorinert (FC 70:FC 77 = 1:1), in a nonmagnetic high-pressure clamp

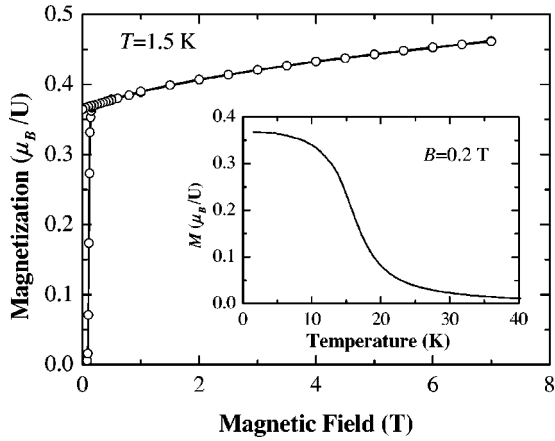


FIG. 1. Magnetization curve of single-crystalline $\text{UCo}_{0.98}\text{Fe}_{0.02}\text{Al}$ along the c axis for an ambient pressure at 1.5 K. Inset: temperature dependence of the magnetization in the field of 0.2 T.

cell made of a Ti-Cu alloy. The pressure exerted on the sample at low temperatures was calibrated by measuring the temperature of the superconducting transition in Pb. The total magnetization of the sample and the surrounding high-pressure cell was measured with an extraction-type magnetometer in magnetic fields up to 7 T produced by a superconducting magnet. Although the magnetization of the high-pressure cell is extremely small, it was subtracted from the total magnetization to obtain the intrinsic magnetization value of the sample.

III. EXPERIMENTAL RESULTS

In contrast to the paramagnetic ground state of UCoAl , the $\text{UCo}_{0.98}\text{Fe}_{0.02}\text{Al}$ compound was found to become ferromagnetic at ambient pressure. Figure 1 shows the magnetization curve of $\text{UCo}_{0.98}\text{Fe}_{0.02}\text{Al}$ measured at 1.5 K in a magnetic field applied along the c axis. (In magnetic fields applied along the c plane, the sample behaves as a Pauli paramagnet and no metamagnetic transition was observed down to the lowest temperature.) The magnetization process exhibits a hysteresis. For the thermally demagnetized sample (cooled in zero field) the initial susceptibility is relatively low ($0.05\mu_B/\text{T}$) for a field interval below a starting field $B_{st} \approx 0.1$ T. Domain walls begin to move through the crystal only at B_{st} , but the magnetization reaches the spontaneous magnetization value in a rather narrow field interval. The hysteresis loop is almost rectangular with a nearly 100% remanent magnetization. A similar hysteresis behavior was observed for other ferromagnetic U compounds with a ZrNiAl-type structure, which was attributed to the pinning of the narrow domain walls in highly anisotropic crystals.³ In high fields, the magnetization does not saturate but shows a strong increase with increasing field, similar to the case of UCoAl in magnetic fields above the metamagnetic transition. The temperature dependence of the magnetization in a small field (the inset in Fig. 1) is typical of a ferromagnet. The value of the Curie temperature $T_C = 18$ K was estimated from the extrapolation of the $M^2(T)$ curve to $M=0$. The T_C

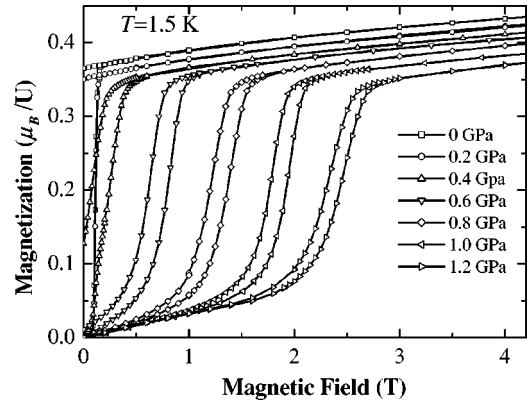


FIG. 2. Magnetization curves of $\text{UCo}_{0.98}\text{Fe}_{0.02}\text{Al}$ at 1.5 K measured in both increasing and decreasing fields for different pressures.

value determined from the Arrott plots M^2 versus H/M is 16 K. However, the Arrott plots are strongly nonlinear around T_C , indicating that the ferromagnetic state is very close to an instability.

The magnetization curves measured for $\text{UCo}_{0.98}\text{Fe}_{0.02}\text{Al}$ at 1.5 K at various pressures are shown in Fig. 2. The ferromagnetism is destabilized and the metamagnetic transition appears at pressures above 0.4 GPa. The critical field of the transition B_c is defined as the field at which the differential susceptibility dM/dB reaches the maximum value. A hysteresis of the critical field $\Delta B_c \sim 0.15$ T indicates that the metamagnetic transition in $\text{UCo}_{0.98}\text{Fe}_{0.02}\text{Al}$ is of first order. The width of the hysteresis is approximately three times larger than that for the parent compound UCoAl .

The average critical field B_c is plotted as a function of pressure in Fig. 3(a). The value of B_c increases linearly for $P > 0.4$ GPa with a pressure derivative $dB_c/dP = 2.8$ T/GPa. This value is only slightly larger than 2.62 T/GPa reported for UCoAl .⁹ A much stronger pressure effect on the metamagnetic transition with $dB_c/dP = 5$ T/GPa was reported for polycrystalline $\text{U}_{0.98}\text{Y}_{0.02}\text{CoAl}$, where the ground state at ambient pressure consists of the mixture of ferromagnetic and metamagnetic moments.²⁰ From the $B_c(P)$ dependence, the critical pressure for the onset of metamagnetism in $\text{UCo}_{0.98}\text{Fe}_{0.02}\text{Al}$ is determined to be $P_c = 0.33$ GPa. From the linear extrapolation of the $M(B)$ dependences for the paramagnetic and the induced ferromagnetic state to $B = B_c$, we determined the change of the magnetization at the critical field ΔM (for the ferromagnetic magnetization curves it corresponds to the spontaneous magnetic moment M_s). The value of ΔM gradually decreases with increasing pressure [Fig. 3(b)], similarly to that of 3d itinerant electron metamagnets.¹²

Figure 4(a) shows the temperature evolution of the magnetization curves of $\text{UCo}_{0.98}\text{Fe}_{0.02}\text{Al}$ at a pressure of 0.3 GPa, which is just below the P_c value. The ground state is ferromagnetic, however, the metamagnetic component appears with increasing temperature, which is especially evident for the magnetization curves measured at temperatures between 10 and 14 K. From the $B_c(T)$ dependence we have determined the transition temperature from the ferromagnetic to

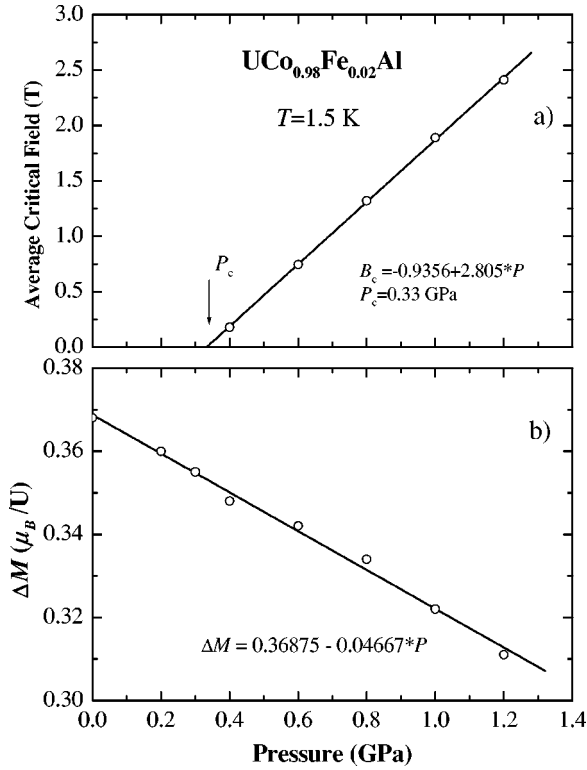


FIG. 3. Average critical field of the metamagnetic transition (a) and the change of the magnetization at the transition ΔM (b) at 1.5 K as functions of pressure.

the metamagnetic state to be $T_1 = 5.7 \text{ K}$ for the external pressure of 0.3 GPa. The first-order temperature-induced transition from the ferromagnetic phase to metamagnetic phase was predicted by the theoretical magnetic phase diagram for isotropic systems¹² and observed earlier in $3d$ itinerant electron systems such as $\text{Co}(\text{S}_{1-x}\text{Se}_x)_2$ (Ref. 21) and $\text{La}(\text{Fe}_{1-x}\text{Si}_x)_{13}$.²² We are convinced that the present experimental result on $\text{UCo}_{0.98}\text{Fe}_{0.02}\text{Al}$ provides clear experimental evidence of the existence of such a transition in $5f$ itinerant electron systems.

For the pressure range where the metamagnetism is observable, the transition becomes gradually broadened with increasing temperature. As an example, in Fig. 4(b) we show the magnetization curves at various temperatures for $P = 1.2 \text{ GPa}$. The S shape of the magnetization curve disappears only above 20 K. In order to determine the critical temperature T_0 at which the first-order metamagnetic transition disappears, in Fig. 5(a) we plot the temperature dependence of the hysteresis width of the critical field ΔB_c . For $P = 0.4 \text{ GPa}$, the value of ΔB_c decreases with increasing temperature and vanishes at $T_0 \sim 12 \text{ K}$. A similar value of T_0 was determined for UCoAl at ambient pressure, when the B_c value is approximately the same. Unfortunately, we cannot use the same way to determine critical temperature T_0 at higher pressures because the $\Delta B_c(T)$ dependence is strongly nonlinear and the hysteresis above 5 K becomes very small. For UCoAl the value of dM/dB at the critical field decreases sharply around the temperature where ΔB_c becomes zero.⁹ The temperature dependences of the dM/dB derivative at

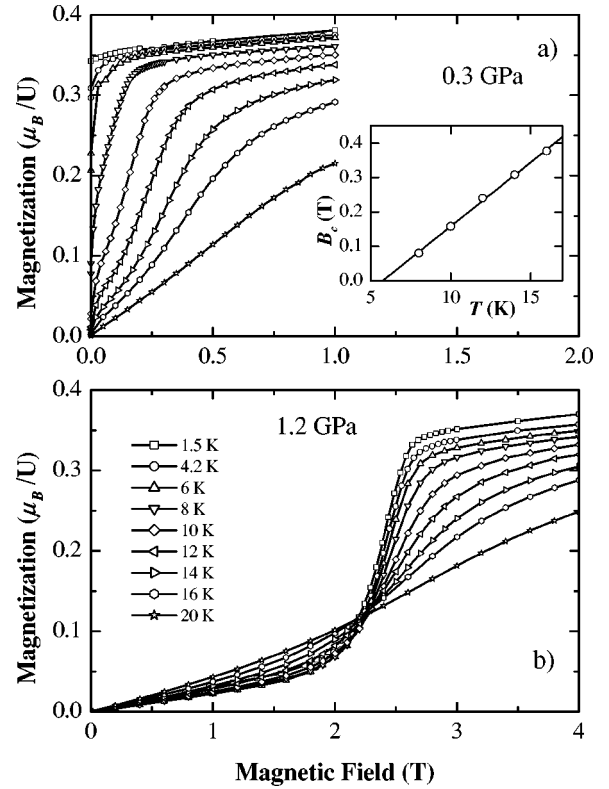


FIG. 4. Magnetization curves of $\text{UCo}_{0.98}\text{Fe}_{0.02}\text{Al}$ for 0.3 GPa (field-down measurements) and 1.2 GPa (averaged field-up and field-down measurements) at different temperatures. Inset: temperature dependence of the critical field for 0.3 GPa.

$B = B_c$ for $\text{UCo}_{0.98}\text{Fe}_{0.02}\text{Al}$ are shown in Fig. 5(b). For $P = 0.4 \text{ GPa}$, the T_0 value determined from $\Delta B_c(T)$ dependence corresponds to the temperature at the steepest decrease of $dM/dB(T)$. At this temperature, dM/dB amounts to half of its ground state value. In order to estimate the pressure change of T_0 , we consider T_0 as the temperature at which the dM/dB value is a half of that for 1.5 K. Thus the determined value of T_0 decreases slightly with increasing pressure down to 10 K at 1.2 GPa.

For itinerant electron metamagnets, the B_c value increases quadratically with temperature ($B_c \sim T^2$). Such dependences were observed for Laves phase compounds [e.g., YCo_2 and $\text{Co}(\text{S}_{1-x}\text{Se}_x)_2$] (Ref. 23) and for itinerant $5f$ -electron metamagnets based on UCoAl .^{9,24} The average critical field of $\text{UCo}_{0.98}\text{Fe}_{0.02}\text{Al}$ is plotted in Fig. 6 as a function of the squared temperature for different pressures. The critical field increases nearly linearly with T^2 for all the pressures. A small nonlinearity and difference in the slope of $B_c(T^2)$ for $P = 0.4 \text{ GPa}$ may originate from the contribution of some amount of the ferromagnetic phase with its own hysteresis, which can survive at this pressure.

The temperature dependences of the susceptibility of itinerant electron metamagnets always show a broad maximum near the temperature where the S shape of the magnetization curves disappears.² This phenomenon is predicted by the theory of itinerant electron metamagnets based on the spin-fluctuation model.²⁵ For UCoAl , a very clear susceptibility maximum was observed at $T_{\text{max}} \sim 20 \text{ K}$.⁹ Figure 7 shows the

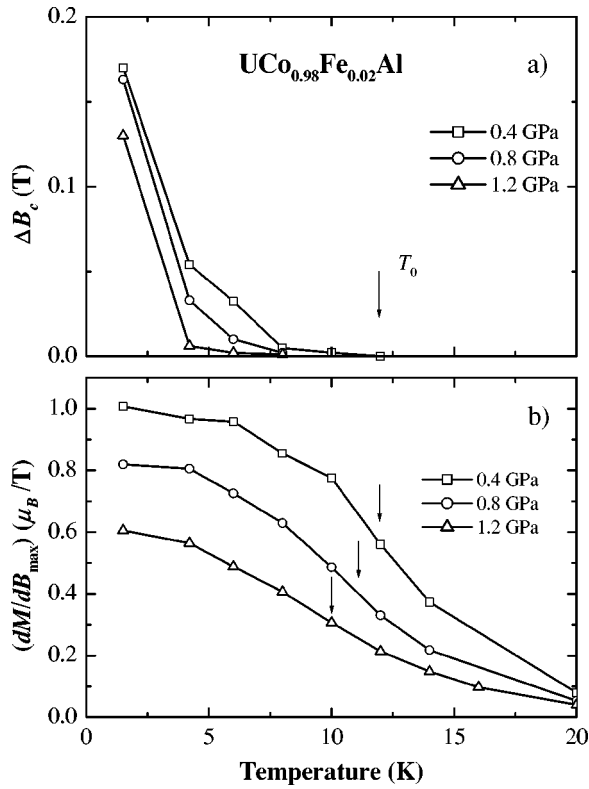


FIG. 5. Width of the hysteresis of the metamagnetic transition ΔB_c (a) and the slope of the magnetization curve dM/dB at $B = B_c$ (b) as functions of temperature for various pressures.

temperature dependence of the susceptibility of $\text{UCo}_{0.98}\text{Fe}_{0.02}\text{Al}$ in a field 0.2 T at various pressures. It is seen that the susceptibility decreases with increasing pressure and a broad maximum of the susceptibility appears under the pressure above 0.6 GPa. At 0.4 GPa, the susceptibility maximum is masked by a large susceptibility contribution that originates from the ferromagnetic component and decreases with increasing temperature. The low-temperature upturn of the susceptibility below 8 K indicates that the sample is not completely homogeneous and that some ferromagnetic component exists even at the maximum applied pressure 1.2

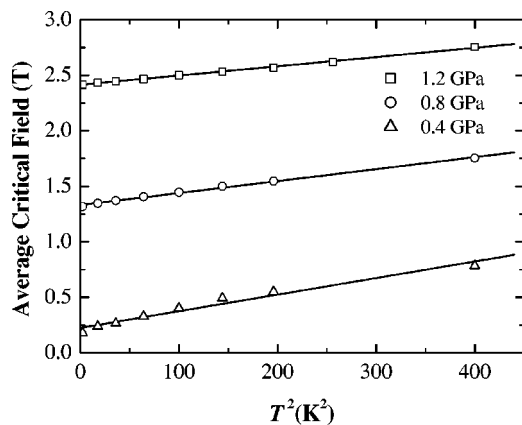


FIG. 6. Average critical field B_c as a function of squared temperature for various pressures.

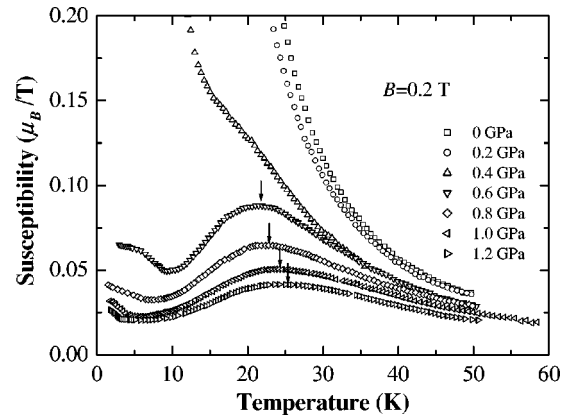


FIG. 7. Temperature dependences of the susceptibility χ of $\text{UCo}_{0.98}\text{Fe}_{0.02}\text{Al}$ measured in a magnetic field of 0.2 T at different pressures.

GPa. The temperature of the susceptibility maximum T_{max} is close to that of the parent compound UCoAl . The value of T_{max} increases with increasing pressure. For itinerant electron metamagnets, a rather good proportionality holds between the values of B_c for $T = 0$ K and T_{max} .^{2,23} As shown in Fig. 8, a linear relation between B_c and T_{max} holds also in $\text{UCo}_{0.98}\text{Fe}_{0.02}\text{Al}$. The estimated slope of $dB_c/dT_{\text{max}} = 0.48$ T/K is larger than 0.36 T/K reported for UCoAl .⁹

Figure 9 shows the magnetic phase diagram of $\text{UCo}_{0.98}\text{Fe}_{0.02}\text{Al}$ in the P - T plane. At low pressure and low temperature the compound is ferromagnetic. With increasing temperature, the ferromagnetic phase is destabilized. For the low-pressure region, the second-order type transition to the paramagnetic state occurs at $T = T_C$. For a narrow pressure range $\sim 0.25 \leq P \leq 0.33$ GPa the compound shows a first-order transition to the metamagnetic phase at $T = T_1$. The paramagnetic ground state with the metamagnetic transition appears in the region above ~ 0.33 GPa and below the T_0 line. At the temperature above T_0 the sample is paramagnetic, but the S-shape of the magnetization curve is observed up to $T \sim T_{\text{max}}$. The observed magnetic phase diagram is similar to the calculated diagram for isotropic itinerant metamagnets.^{2,12}

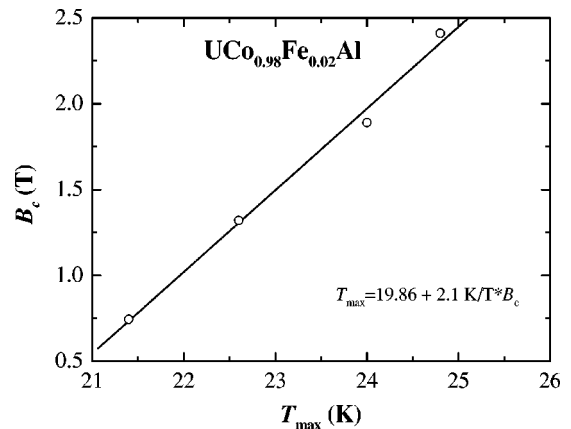


FIG. 8. Critical field of the metamagnetic transition B_c at 1.5 K as a function of temperature of the susceptibility maximum T_{max} at various pressures.

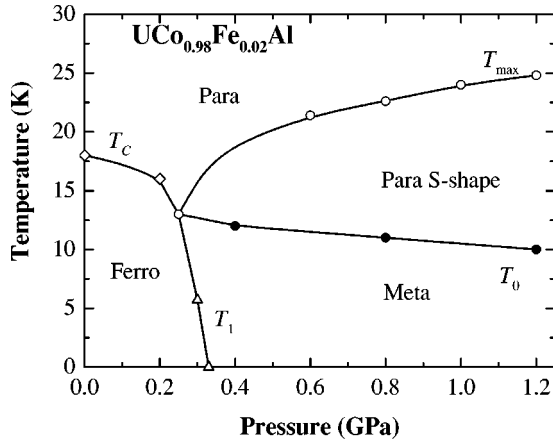


FIG. 9. Magnetic phase diagram of $\text{UCo}_{0.98}\text{Fe}_{0.02}\text{Al}$ in the P - T plane.

IV. DISCUSSION

The magnetization curve for an itinerant metamagnet can be described by the following magnetic equation of state:

$$B = a_0 M + b_0 M^3 + c_0 M^5, \quad (1)$$

where B is the magnetic field (magnetic induction) in terms of T, M is the uniform magnetization in terms of μ_B/U . The Landau expansion coefficients a_0 , b_0 , and c_0 are the functions of the electron density of states and its derivatives at the Fermi level. The metamagnetic transition appears under the conditions:²⁵

$$a_0 > 0, \quad b_0 < 0, \quad c_0 > 0, \quad \text{and} \quad \frac{3}{16} < \frac{a_0 c_0}{b_0^2} < \frac{9}{20}, \quad (2)$$

where $M(B)$ in Eq. (1) becomes a triple-valued function. In the equilibrium condition, the metamagnetic transition occurs at a critical field B_c , for which the free energies of the paramagnetic and ferromagnetic states, respectively, are equal. Equation of states (1) suggests that the magnetization tends to saturate in high fields. For UCoAl -type metamagnets, the magnetization shows no tendency to saturate in fields above the metamagnetic transition. In order to describe the non-saturated magnetization curve we must take into account an additional paramagnetic contribution χ_0 , assuming it to be independent of temperature, magnetic field and pressure.⁹ The coefficient a_0 in Eq. (1) is the inverse susceptibility and can be determined directly from the experiment. However, the low-temperature susceptibility of $\text{UCo}_{0.98}\text{Fe}_{0.02}\text{Al}$ is enhanced by a small ferromagnetic component (see Fig. 7). For UCoAl , the susceptibility increases with temperature proportional to $\sim T^2$ at low temperatures. The spin-fluctuation theory gives the following expression for the temperature dependence of the susceptibility of the strongly anisotropic ferromagnet:

$$\chi(T)^{-1} = a(T) = a_0 + 3b_0 Q(T) + 15c_0 Q(T)^2, \quad (3)$$

where $Q(T)$ is the mean-square amplitude of longitudinal fluctuations of magnetization parallel to B along the c axis.¹⁰ Under condition (2), the susceptibility increases with in-

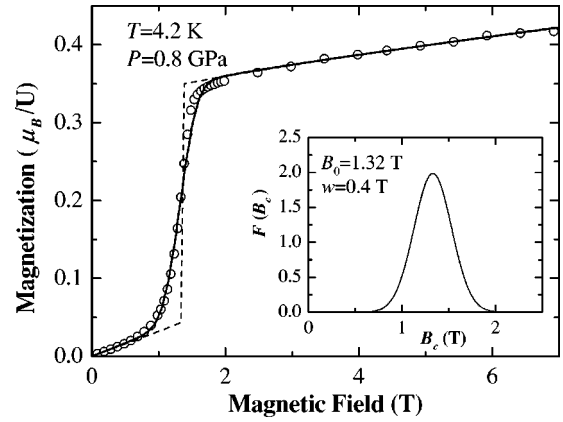


FIG. 10. Magnetization curves of $\text{UCo}_{0.98}\text{Fe}_{0.02}\text{Al}$ for $T = 4.2$ K at $P = 0.8$ GPa: experiment (symbols), calculation using Eq. (1) (dashed line), and calculation with the distribution function shown in the inset (solid line).

creasing T at low temperatures where $Q(T)$ is also proportional to T^2 ,²⁵ then reaches the maximum and decreases at high temperatures. In order to determine a correct value of the ground-state susceptibility $\chi(0)$ of the metamagnetic $\text{UCo}_{0.98}\text{Fe}_{0.02}\text{Al}$ phase, we subtracted the low-temperature upturn of the susceptibility from the experimental $\chi(T)$ curves (Fig. 7). The relation then gives the expansion coefficient a_0 :

$$a_0 = [\chi(0) - \chi_0]^{-1}. \quad (4)$$

We described the metamagnetic magnetization curves using Eq. (1) by varying only expansion coefficients b_0 and c_0 . The value of the additional paramagnetic susceptibility χ_0 , which allows to obtain the best fitting results for all pressures, was chosen as $0.007\mu_B/\text{T}$, slightly smaller than $\chi_0 = 0.011\mu_B/\text{T}$ estimated for UCoAl .⁹ As an example, Fig. 10 shows the experimental magnetization curve (circles) and the fitted curve (dashed line) of $\text{UCo}_{0.98}\text{Fe}_{0.02}\text{Al}$ under the pressure 0.8 GPa at 4.2 K, where the initial susceptibility is not affected by the ferromagnetic impurity. Both the low- and high-field parts of the magnetization curve are fitted well, but the difference occurs between the experimental and calculated magnetizations, respectively, near the metamagnetic transition. The experimental metamagnetic transition is broadened, most likely because of the nonhomogeneous (or, at least, statistical) distribution of the alloying element Fe. The coincidence between the experiment and the model can be substantially improved by taking into account a Gaussian normal distribution of the critical fields,

$$F(B_c) = \frac{1}{w\sqrt{\pi/2}} \exp\left[-2\frac{(B_c - B_0)^2}{w^2}\right], \quad (5)$$

where B_0 is the average critical field that corresponds to the maximum of dM/dB , and w is the half-width of the distribution. As a rule, the Gaussian-type distributions describe well the composition fluctuations in the substituted com-

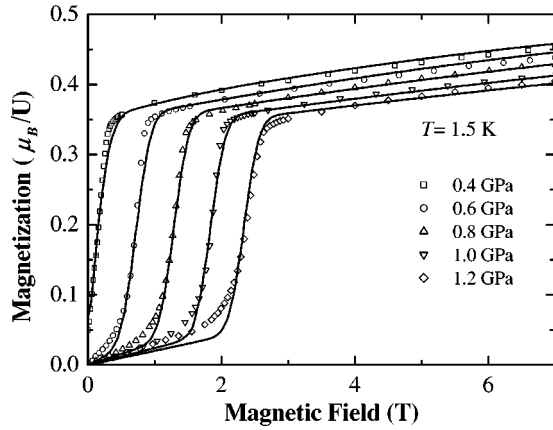


FIG. 11. Magnetization curves of $\text{UCo}_{0.98}\text{Fe}_{0.02}\text{Al}$ for $T = 1.5$ K at different pressures: experiment (open symbols), calculation using Eq. (1), and the distribution function (solid line).

pounds (see, e.g., Ref. 26). The solid line in Fig. 10 represents the calculated magnetization curve with the distribution function shown in the inset.

Figure 11 shows the calculated magnetization curves at 1.5 K for different pressures. They reproduce well the high-field magnetization and the critical field of the metamagnetic transition. A difference is observed in the low-field region, where, as discussed above, the susceptibility is enhanced by a ferromagnetic contribution. It should be noted that the magnetization curves for all pressures are described well with the same half-width of the distribution function, $w = 0.35$ T for 1.5 K.

The uncertainty in determination of the coefficients a_0 , b_0 , and c_0 for $\text{UCo}_{0.98}\text{Fe}_{0.02}\text{Al}$ at 0.4 GPa is larger compared to that at the higher pressures because of the presence of a weak ferromagnetic contribution. In this case we cannot determine the coefficient a_0 from the experimental initial susceptibility. Therefore we determined a_0 at 0.4 GPa using $a_0(P)$ dependence for $P \geq 0.6$ GPa, which is found to be nearly linear. Then b_0 and c_0 coefficients can be easily obtained by a simultaneous fitting of the values of B_c and the magnetization above the metamagnetic transition. Since the B_c value is lower than the width of the distribution function, the calculated magnetization curve for $P = 0.4$ GPa shown in Fig. 11 displays a weak ferromagnetism, which is actually due to a mixture of the ferromagnetic and paramagnetic ground states of different microscopic areas of the inhomogeneous $\text{UCo}_{0.98}\text{Fe}_{0.02}\text{Al}$ sample.

The values of the coefficients a_0 , b_0 and c_0 are plotted in Fig. 12 as functions of pressure. All the absolute values of the three coefficients monotonically decrease with decreasing pressure. The a_0 coefficient tends to change the sign at a pressure ~ 0.22 GPa. This implies that $\text{UCo}_{0.98}\text{Fe}_{0.02}\text{Al}$ at ambient pressure is a conventional ferromagnet with $a_0 < 0$. The values of $a_0 c_0 / b_0^2$ fall between 0.20 and 0.23 for all the pressures in the range of metamagnetism, in agreement with condition (2). The pressure dependence of $a_0 c_0 / b_0^2$ is strongly nonlinear. The ferromagnetic state appears for $P = 0.33$ GPa when the coefficient a_0 is still positive and $a_0 c_0 / b_0^2$ becomes equal to $3/16 = 0.1875$.

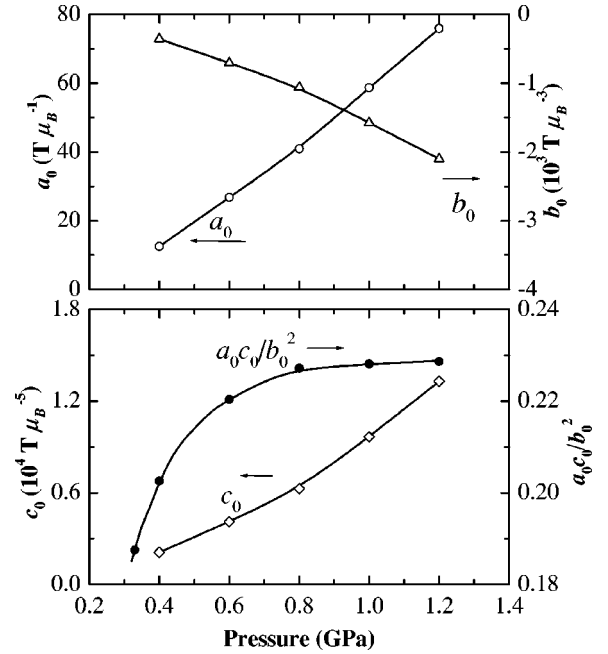


FIG. 12. Pressure variations of the Landau expansion coefficients a_0 , b_0 , c_0 and the value of $a_0 c_0 / b_0^2$ at 1.6 K.

In the theory of itinerant electron metamagnets with strong anisotropy, the susceptibility value at T_{\max} can be estimated using the values of a_0 , b_0 , and c_0 , determined from the magnetization curve at $T = 1.6$ K as⁹

$$\chi(T_{\max})^{-1} = a(T_{\max}) = a_0 - \frac{3}{20} \frac{b_0^2}{c_0}. \quad (6)$$

Figure 13 shows the calculated values of $\chi^{-1}(T_{\max})$ for various pressures, which are compared with the experimental ones $\{= [\chi_{\text{exp}}(T_{\max}) - \chi_0]^{-1}\}$ for $\text{UCo}_{0.98}\text{Fe}_{0.02}\text{Al}$. Both the experimental and theoretical values increase linearly with pressure, however, they differ approximately by two times. Similar dependences for UCoAl compare well with each

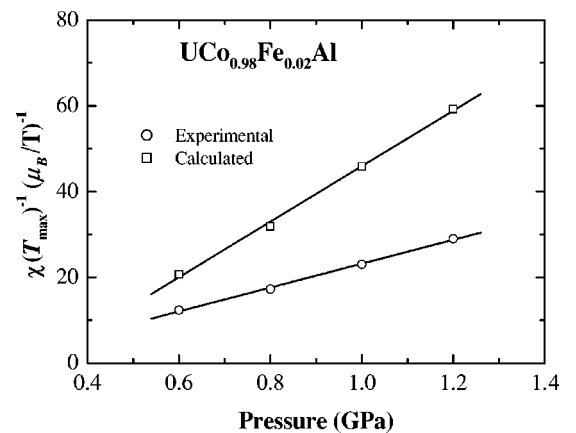


FIG. 13. Values of the inverse susceptibility of $\text{UCo}_{0.98}\text{Fe}_{0.02}\text{Al}$ for $T = T_{\max}$ as a function of external pressure. The circles indicate the experimental data, and squares are the values calculated with the coefficients a_0 , b_0 , and c_0 derived from the magnetization curves for 1.6 K.

other,⁹ that provides evidence of the applicability of the spin-fluctuation theory to the strongly anisotropic itinerant metamagnets. The smaller experimental $\chi^{-1}(T_{\max})$ values in comparison with those predicted by the spin-fluctuation theory can be caused by the enhancement of the susceptibility because of the presence of a ferromagnetic component in the metamagnetic sample. Indeed, the enhanced susceptibility was also observed for an off-stoichiometric single crystal $U_{0.9}Co_{1.05}Al_{1.05}$ (Ref. 24) that exhibits a broadened metamagnetic transition and contains some ferromagnetic component at ambient pressure.

According to the Eq. (6), the susceptibility at T_{\max} becomes infinite at $a_0c_0/b_0^2=3/20$ that corresponds to the triple point of the magnetic phase diagram, which is the boundary between the first- and second-order transitions.¹¹ The inverse susceptibility shown in Fig. 13 is a linear function of the pressure. The pressure that corresponds to the triple point in the magnetic phase diagram in Fig. 9 is determined to be ~ 0.25 GPa. It should be noted that in our estimation the coefficient a_0 changes the sign just below the triple point.

The magnetic phase diagrams reported in the works^{2,12} were calculated for the isotropic itinerant electron metamagnets. For the strongly anisotropic metamagnets such as UCoAl, the calculated magnetic phase diagram is expected to be slightly different. At a finite temperature T , the coefficients a_0 , b_0 , and c_0 in Eq. (1) are renormalized by thermal spin fluctuations, and the magnetic equation of state is given by

$$B = a(T)M + b(T)M^3 + c(T)M^5, \quad (7)$$

where the coefficients $a(T)$, $b(T)$, and $c(T)$ are functions of a_0 , b_0 , and c_0 and the thermal average of the fluctuating magnetic moment. The expression for $a(T) = \chi^{-1}(T)$ is given by Eq. (3), and the expressions for $b(T)$ and $c(T)$ are written by

$$b(T) = b_0 + 10c_0Q(T), \quad (8)$$

$$c(T) = c_0. \quad (9)$$

For simplicity, we neglect the temperature dependence of c in the theory. However, the observed results for UCoAl exhibit a temperature dependence of c .^{9,10}

The equations of the phase boundary lines can be obtained from conditions (2) by replacing the ground-state expansion coefficients a_0 , b_0 , and c_0 with the temperature-dependent parameters $a(T)$, $b(T)$, and $c(T)$. From these relations, the mean-square amplitude of longitudinal fluctuations of the magnetization along the c axis $Q(T)$ at the critical temperature T_0 of the disappearance of the metamagnetic transition can be determined as

$$Q(T_0) = \frac{|b_0|}{10c_0} \left(1 - \sqrt{\frac{10}{3}} \sqrt{\frac{a_0c_0}{b_0^2} - \frac{3}{20}} \right). \quad (10)$$

The ferromagnetic state appearing at $a(T)c(T)/b(T)^2 = 3/16$ becomes unstable and a first-order transition occurs at the critical temperature T_1 at which

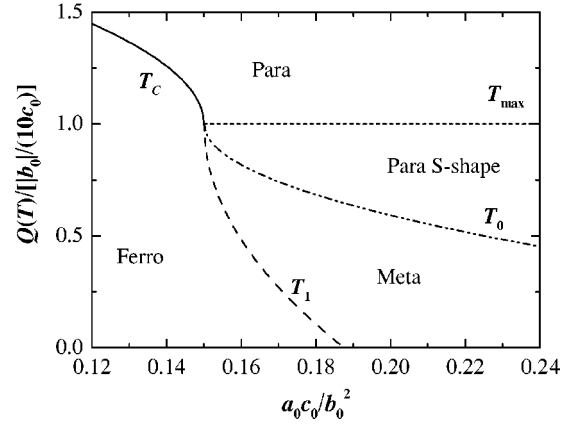


FIG. 14. Theoretical magnetic phase diagram for strongly anisotropic itinerant electron compounds. Curves denoted as (T_C) , (T_1) , (T_0) , and (T_{\max}) show respectively $Q(T_C)$, $Q(T_1)$, $Q(T_0)$ and $Q(T_{\max})$, scaled by $|b_0|/10c_0$.

$$Q(T_1) = \frac{|b_0|}{10c_0} \left(1 - \sqrt{\frac{80}{3}} \sqrt{\frac{a_0c_0}{b_0^2} - \frac{3}{20}} \right). \quad (11)$$

The maximum of $\chi(T)$ dependence is given by the relation $\partial\chi(T)^{-1}/\partial Q(T) = 0$, and we obtain

$$Q(T_{\max}) = \frac{|b_0|}{10c_0}. \quad (12)$$

Finally, the condition of the second-order transition from the ferromagnetic to the paramagnetic state at T_C is given by

$$a(T_C) = 0, \quad b(T_C) > 0, \quad (13)$$

and from Eq. (3) we can easily obtain

$$Q(T_C) = \frac{|b_0|}{10c_0} \left(1 + \sqrt{1 - \frac{20}{3} \frac{a_0c_0}{b_0^2}} \right). \quad (14)$$

The magnetic phase diagram with the phase boundaries corresponding to Eqs. (10)–(12) and (14) is plotted in Fig. 14. As $Q(T)$ is a monotonically increasing function of temperature, the vertical axis corresponds to the temperature. On the other hand, the a_0c_0/b_0^2 ratio varies monotonically with pressure (Fig. 12). Therefore, the horizontal axis corresponds to the pressure. The experimental magnetic phase diagram of Fig. 9 is consistent with the calculated one, implying the applicability of the spin-fluctuation theory to the strongly anisotropic $5f$ itinerant electron metamagnets.

According to the theory of anisotropic itinerant electron metamagnets, the critical field of the metamagnetic transition is given by⁹

$$B_c \cong \frac{3}{4} \sqrt{\frac{|b_0|}{3c_0}} \left(a_0 - \frac{3}{16} \frac{b_0^2}{c_0} + \frac{3}{4} |b_0| Q(T) \right) \quad (15)$$

in the first-order approximation of $Q(T)$. Since $Q(T)$ is positive and proportional to T^2 at low temperature, the value of $B_c(T)$ increases with temperature as T^2 ,

$$B_c = B_c(0) + \beta T^2, \quad (16)$$

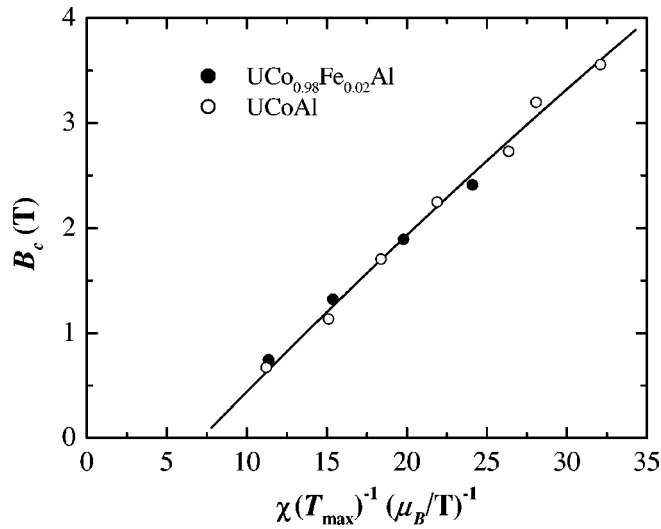


FIG. 15. The critical field of the metamagnetic transition at 1.5 K vs the inverse susceptibility at T_{\max} for $\text{UCo}_{0.98}\text{Fe}_{0.02}\text{Al}$ (●) and UCoAl (○).

in agreement with the experimental results, as shown in Fig. 6.

Substituting Eqs. (6) and (12) into Eq. (15), we get the relation between B_c at 0 K and the susceptibility at T_{\max} :

$$B_c(0) = \frac{5\sqrt{30}}{16} \sqrt{Q(T_{\max})} \left[\chi(T_{\max})^{-1} - \frac{1}{5} a_0 \right]. \quad (17)$$

Saito *et al.*²⁷ found a universal linear relation between the critical field and the inverse susceptibility for isotropic Laves-phase metamagnets. Figure 15 shows B_c versus $\chi(T_{\max})^{-1}$ dependences for $\text{UCo}_{0.98}\text{Fe}_{0.02}\text{Al}$ and UCoAl .⁹ For both compounds the dependences follow a straight solid line. However, the slope of the line is found to be about $0.14\mu_B/\text{U}$, considerably lower than the reported value of $0.4\mu_B/\text{Co}$ for isotropic Laves phase compounds.²⁷ For the isotropic metamagnets, a numerical coefficient for a_0 in Eq. (15) is about four times smaller^{25,27} (1/21 in comparison with 1/5 for anisotropic metamagnets), and the change of a_0 gives a small contribution to the change of $B_c(0)$. For anisotropic UCoAl -type metamagnets, the a_0 coefficient changes considerably by the application of pressure, and the $B_c(0)$ value is affected by both components in the square brackets of the Eq. (15). Fortunately, both $\chi(T_{\max})^{-1}$ and a_0 increase linearly with increasing pressure, so the linearity of the dependence of $B_c(0)$ on $\chi(T_{\max})^{-1}$ holds for UCoAl -type systems.

Finally, we discuss the change in the γ -value of the electronic specific heat due to the metamagnetic transition. According to Ref. 28, the change of γ can be estimated as

$$\Delta\gamma = -2\beta\Delta M, \quad (18)$$

where ΔM is the change of the magnetization at the critical field [Fig. 3(b)] and the coefficient β is given by Eq. (16). The estimation gives $\Delta\gamma = -4.1 \text{ mJ mol}^{-1} \text{ K}^{-2}$ for the metamagnetic transition at 0.6 GPa. The specific-heat measurements of polycrystalline UCoAl indicate that the γ -value changes from $70 \text{ mJ mol}^{-1} \text{ K}^{-2}$ in zero field to $62 \text{ mJ mol}^{-1} \text{ K}^{-2}$ at 5 T,⁷ consistent with our estimations. The absolute value of $\Delta\gamma$ decreases nearly linear with increasing pressure. At $P = 1.2 \text{ GPa}$, we have $\Delta\gamma = -2.9 \text{ mJ mol}^{-1} \text{ K}^{-2}$. These results suggest that the spin fluctuations in $\text{UCo}_{0.98}\text{Fe}_{0.02}\text{Al}$ are suppressed by the application of high pressure.

V. CONCLUSION

We performed a study of the magnetic properties of the $\text{UCo}_{0.98}\text{Fe}_{0.02}\text{Al}$ compound, which is characterized by itinerant $5f$ electrons, under hydrostatic pressure. The ground state is ferromagnetic at ambient pressure, but the spontaneous moment vanishes and the UCoAl -type metamagnetism in fields applied along the c axis appears at $P \geq 0.4 \text{ GPa}$. The critical field of the metamagnetic transition increases with pressure at a rate of 2.8 T/GPa. In the metamagnetic state, the temperature dependence of the susceptibility shows a broad maximum at a temperature T_{\max} . The susceptibility decreases and the value of T_{\max} gradually increases with pressure, similar to these for UCoAl . Using the experimental data, we plotted the magnetic phase diagram in the P - T plane. Based on the theory of itinerant electron metamagnetism extended to the case of anisotropic thermal fluctuations of the magnetic moment, we obtained the calculated magnetic phase diagram for anisotropic itinerant electron metamagnets, consistent with the experimental phase diagram. The observed susceptibility maximum, the pressure dependence of the inverse susceptibility at T_{\max} , and the temperature dependence of B_c can also be explained by the theory.

ACKNOWLEDGMENTS

This work was supported by a Grant-in Aid for the Scientific Research on Priority Areas (B) from the Ministry of Education, Culture, Sports, Science and Technology of Japan. The stay of N.V.M. at ISSP was also supported by the Ministry. The work was partly supported by the Grant No. 202/02/0739 from the Grant Agency of the Czech Republic.

*Permanent address: Institute of Metal Physics, S. Kovalevskaya 18, 620219 Ekaterinburg, Russia.

†Author to whom correspondence should be addressed. Electronic address: goto@issp.u-tokyo.ac.jp

¹E.P. Wohlfarth and P. Rhodes, *Philos. Mag.* **7**, 1817 (1962).

²T. Goto, K. Fukamichi, and H. Yamaga, *Physica B* **300**, 167 (2001).

³V. Sechovský and L. Havela, in *Handbook of Magnetic Materials*, edited by K. H. J. Buschow (Elsevier, Amsterdam, 1998), Vol. 11, p. 1.

⁴O. Eriksson, B. Johansson, and M.S.S. Brooks, *J. Phys.: Condens. Matter* **1**, 4005 (1989).

⁵M. Wulff, J.M. Fournier, A. Delapalme, B. Gillon, V. Sechovský, L. Havela, and A.V. Andreev, *Physica B* **163**, 331 (1990).

⁶A.V. Andreev, R.Z. Levitin, Y.F. Popov, and R.Y. Yumaguzhin, *Fiz. Tverd. Tela (Leningrad)* **27**, 1902 (1985) [*Sov. Phys. Solid State* **27**, 1145 (1985)].

⁷V. Sechovský, L. Havela, F.R. de Boer, J.J.M. Franse, P.A. Veenhuizen, J. Sebek, J. Stehno, and A.V. Andreev, *Physica B* **142**, 283 (1986).

- ⁸A.V. Andreev, M.I. Bartashevich, T. Goto, K. Kamishima, L. Havela, and V. Sechovský, *Phys. Rev. B* **55**, 5847 (1997).
- ⁹N.V. Mushnikov, T. Goto, K. Kamishima, H. Yamada, A.V. Andreev, Y. Shiokawa, A. Iwao, and V. Sechovský, *Phys. Rev. B* **59**, 6877 (1999).
- ¹⁰H. Yamada, N.V. Mushnikov, and T. Goto, *Physica B* **281-282**, 218 (2000).
- ¹¹H. Yamada, N.V. Mushnikov, and T. Goto, *J. Phys. Chem. Solids* **63**, 1189 (2002).
- ¹²H. Yamada, K. Fukamichi, and T. Goto, *Phys. Rev. B* **65**, 024413 (2001).
- ¹³A.V. Andreev, I.K. Kozlovskaya, N.V. Mushnikov, T. Goto, V. Sechovský, L. Havela, Y. Homma, and Y. Shiokawa, *J. Magn. Magn. Mater.* **196-197**, 658 (1999).
- ¹⁴A.V. Andreev, V. Sechovský, D. Rafaja, L. Dobiášová, Y. Homma, and Y. Shiokawa, *J. Alloys Compd.* **307**, 77 (2000).
- ¹⁵A.V. Andreev, Y. Homma, Y. Shiokawa, and V. Sechovský, *J. Alloys Compd.* **269**, 34 (1998).
- ¹⁶A.V. Andreev, V. Sechovský, N.V. Mushnikov, T. Goto, Y. Homma, and Y. Shiokawa, *J. Alloys Compd.* **306**, 72 (2000).
- ¹⁷A.V. Andreev, H. Aruga Katori, and T. Goto, *J. Alloys Compd.* **224**, 117 (1995).
- ¹⁸V.H. Tran, R. Troc, A. Zaleski, F.G. Vagizov, and H. Drulis, *Phys. Rev. B* **54**, 15 907 (1996).
- ¹⁹A.V. Andreev, N.V. Mushnikov, T. Goto, and V. Sechovský, *Phys. Rev. B* **60**, 1122 (1999).
- ²⁰A.V. Andreev, M. Kosaka, Y. Uwatoko, and V. Sechovský, *J. Alloys Compd.* **309**, 45 (2000).
- ²¹T. Goto, Y. Shindo, H. Takahashi, and S. Ogawa, *Phys. Rev. B* **56**, 14 019 (1997).
- ²²A. Fujita, Y. Akamatsu, and K. Fukamichi, *J. Appl. Phys.* **85**, 4756 (1999).
- ²³N. H. Duc and T. Goto, in *Handbook on the Physics and Chemistry of Rare Earths*, edited by K. A. Gschneidner, Jr. and L. Eyring (Elsevier, Amsterdam, 1999), Vol. 26, p. 177.
- ²⁴N.V. Mushnikov, A.V. Andreev, T. Goto, and V. Sechovský, *Philos. Mag. B* **81**, 569 (2001).
- ²⁵H. Yamada, *Phys. Rev. B* **47**, 11 211 (1993).
- ²⁶H. Yamada and M. Shimizu, *J. Magn. Magn. Mater.* **104-107**, 1963 (1992).
- ²⁷H. Saito, T. Yokoyama, Y. Terada, K. Fukamichi, H. Mitamura, and T. Goto, *Solid State Commun.* **113**, 447 (2000).
- ²⁸T. Goto, H. Aruga Katori, T. Sakakibara, H. Mitamura, K. Fukamichi, and K. Murata, *J. Appl. Phys.* **76**, 6682 (1994).